Applied Catalysis B: Environmental 108–109 (2011) 54–60

Contents lists available at ScienceDirect

Applied Catalysis B: Environmental

journal homepage: www.elsevier.com/locate/apcatb

Catalytic hydrothermal hydrodenitrogenation of pyridine

Peigao Duan[a,b], Phillip E. Savage[a,*]

[a] Department of Chemical Engineering, University of Michigan, Ann Arbor, MI 48109-2136, USA
[b] College of Physics and Chemistry, Department of Applied Chemistry, Henan Polytechnic University, Jiaozuo 454003, PR China

ARTICLE INFO

Article history:
Received 2 June 2011
Received in revised form 28 July 2011
Accepted 8 August 2011
Available online 17 August 2011

Keywords:
Hydrothermal
Hydrodenitrogenation
Pyridine
$Pt/\gamma\text{-}Al_2O_3$
Supercritical water

ABSTRACT

We herein report on the hydrothermal catalytic conversion of pyridine to hydrocarbons. The catalytic activity of several supported noble metal (5 wt%) catalysts (Pt/C, Pd/C, Ru/C and Rh/C, sulfided Pt/C, and $Pt/\gamma\text{-}Al_2O_3$), a traditional hydrodenitrogenation (HDN) catalyst (sulfided $CoMo/\gamma\text{-}Al_2O_3$), a transition metal carbide (Mo_2C) and sulfide (MoS_2), and a noble metal oxide (PtO_2) toward the HDN of pyridine in a hydrothermal reaction medium between 250 and 400 °C was determined. The $Pt/\gamma\text{-}Al_2O_3$ catalyst proved to be the most active for hydrothermal HDN of pyridine, and we report the effects of batch holding time, reaction temperature, catalyst loading, initial hydrogen pressure, and water density on the $Pt/\gamma\text{-}Al_2O_3$-catalyzed HDN of pyridine in supercritical water. The latter two process variables had the greatest influence on the product yields and distribution. Conditions were identified that lead to essentially 100% conversion of pyridine to N-free hydrocarbons. The catalyst shows some modest loss in activity upon being reused. An HDN reaction network for pyridine under hydrothermal conditions was proposed. The main HDN products are n-butane and n-pentane. Nitrogen was removed as ammonia.

1. Introduction

Microalgae are an attractive complement to lignocellulosic biomass for the production of renewable liquid biofuels. Algae have a higher photosynthetic efficiency, faster growth rate, and higher area-specific yield relative to terrestrial biomass. Processing the wet algal biomass (about 80 wt% water) at 300–350 °C via hydrothermal liquefaction produces a high-energy density crude bio-oil. Unlike crude bio-oils produced from fast pyrolysis of lignocellulosic material, crude bio-oil from hydrothermal liquefaction of algae contains appreciable quantities of nitrogen and sulfur heteroatoms [1–4]. The heteroatom-containing compounds may create problems such as corrosion, poisoning of catalysts during bio-oil upgrading, and production of SO_x and NO_x upon combustion. Therefore, it is desirable to remove the heteroatoms prior to using these renewable biofuels.

S and N removal from petroleum crude oil is done routinely in refineries through heterogeneous catalytic hydrotreating reactions in the presence of high-pressure H_2. Some sulfur source (e.g., H_2S) is often fed along with the oil so that the catalyst remains in its sulfide form, which is the active phase for hydrodenitrogenation (HDN) and hydrodesulfurization (HDS).

Since algal biocrudes produced from hydrothermal liquefaction will be formed in an aqueous environment, it may be advantageous from a process engineering perspective to do HDN and HDS in that same environment. Moreover, there may be advantages to performing heteroatom removal in water above its critical temperature (374 °C). Supercritical water (SCW) behaves like many organic solvents in that small organic compounds are completely miscible [5]. In addition, gaseous reactants, such as H_2, are completely miscible with SCW, which allows high concentrations of gaseous reactants at modest partial pressures. In conventional gas–liquid catalytic reactions, high H_2 pressures are needed to drive the hydrogen into the liquid phase where the reaction occurs but where it is only sparingly soluble. Also, supercritical fluids provide an attractive combination of liquid-like densities, which provide good heat transfer and solubility of potential coke precursors, and gas-like transport properties, which militate against transport processes limiting catalytic reaction rates [6]. Moreover, the HDN and HDS products (hydrocarbons) can be very easily separated from water after the hydrothermal hydrotreating process (e.g., by decanting the cool reactor effluent). Therefore, hydrothermal HDN and HDS may be a path toward nitrogen and sulfur removal from biocrudes produced by hydrothermal liquefaction.

Our previous article [7] on crude algal bio-oil treatment in SCW showed that the SCW reaction medium alone (no catalyst) seemingly provided complete desulfurization of the bio-crude. The abundance of N and O was also considerably reduced in the treated oils, especially in experiments that also included a heterogeneous catalyst. Optimization studies [8] further demonstrated

* Corresponding author at: 3074H.H. Dow Building, 2300 Hayward Street, Ann Arbor, MI 48109, USA. Tel.: +1 734 764 3386; fax: +1 734 763 0459.
E-mail address: psavage@umich.edu (P.E. Savage).

0926-3373/$ – see front matter © 2011 Elsevier B.V. All rights reserved.
doi:10.1016/j.apcatb.2011.08.007

that the catalyst type had the greatest influence on the fraction of N-containing compounds that remained in the treated oil. Thus, there is a need for catalyst screening studies for hydrothermal HDN so that effective catalysts can be identified.

The few previous studies of catalytic heteroatom removal in SCW [9–13] used conventional sulfided CoMo or NiMo hydrotreating catalysts supported on γ-Al_2O_3. These conventional catalysts were effective for heteroatom removal provided H_2 was present. Interestingly, in situ generation of hydrogenating species, by addition of CO or HCOOH rather than H_2, was even more effective than added H_2 itself. Only Yuan et al. [10] reported on hydrothermal catalytic denitrogenation. They did not add H_2 to the reactor, but rather added O_2 so that CO would be formed by partial oxidation followed by H_2 generation through the water gas shift reaction. Adschiri et al. [12] were the first to explore in situ hydrogen generation via partial oxidation of some of the feed material in SCW. The sulfided NiMo catalyst became oxidized with use, however, and its activity declined appreciably on a time scale of a few hours. To our knowledge, there are no published reports regarding the efficacy of other catalysts for hydrothermal catalytic HDN. Ideally, the heterogeneous catalyst would be active for HDN even under oxidizing conditions so that it could be used along with partial oxidation for in situ production of hydrogenating species.

The purpose of this present study is to screen the activity of different potential hydrothermal HDN catalysts and to explore the influence of process variables when using the most active HDN catalyst so identified. We selected pyridine as the heterocyclic nitrogen-containing model compound. Pyridine and its derivatives are present in algal bio-oils [1,7,8]. We report herein on the catalytic effects of several different commercially available materials (5% Pt/C, 5% Pd/C, 5% Ru/C, 5% Rh/C, 5% Pt/C (sulfided), 5% Pt/γ-Al_2O_3, Mo_2C, MoS_2, PtO_2, aluminum oxide, CoMo/γ-Al_2O_3 (sulfided), and activated carbon). We also determined the influence of temperature (380, 400, 420 °C), reaction time (10–150 min), catalyst loading (50–200 wt%), initial hydrogen pressure (0–6.9 MPa), and water density (0.0–0.1 g/cm^3) when using Pt/γ-Al_2O_3 as the hydrothermal HDN catalyst.

2. Experimental

2.1. Materials

CoMo/γ-Al_2O_3 (sulfide with 3.4–4.5 wt% CoO, 11.5–14.5 wt% Mo_2O_3) was obtained from Alfa Aesar. All other chemicals and catalysts were obtained from Sigma–Aldrich in high purity. All chemicals were used as received. The catalyst particle size was around 25 μm. We did not pre-reduce any of the catalysts under H_2 prior to use because we desired to identify catalysts that would be active even when exposed to an oxidizing hydrothermal environment when in use. Freshly deionized water, prepared in house, was used throughout the experiments. Helium, hydrogen, and argon were obtained from Cryogenic Gases. Gas standards for instrument calibration were purchased from Air Liquide Specialty Gases.

We used 316-stainless steel mini-batch reactors equipped with a high-pressure valve that allowed for the recovery and analysis of both the liquid- and gas-phase products in a single run as described in our previous article [7]. The reactor volume was 4.0 cm^3.

2.2. Procedure

Prior to their use in experiments, the reactors were loaded with water and seasoned at 400 °C for 60 min to remove any residual organic material from the reactors and to expose the fresh metal walls to SCW. The reactors were then gradually cooled to ambient temperature and thoroughly washed with acetone and air-dried. We also pressure tested the assembled reactors with helium prior to use.

In a typical run, 0.1 ml of pyridine, the desired amount of catalyst, and 0.4 ml of freshly deionized water were added into the reactor. These loadings result in a water density of 0.10 g/cm^3 at supercritical conditions, and a pyridine/water volume ratio of 1:4. Next, the valve assembly was connected and, the air inside the reactor was displaced with helium by repeatedly applying vacuum (−0.086 MPa) and charging with He (0.14 MPa). All pressures given in this article are gauge pressures. Several helium flushing-vacuum cycles were conducted to ensure the complete removal of air. The reactor was next pressurized to 0.14 MPa with helium (which served as an internal standard for the quantification of gas yields) and then further charged with hydrogen to 5.5 MPa (at room temperature), which results in a H_2/pyridine molar ratio of 6.5:1. After these gases were loaded, the reactor valve was closed and the reactor assembly disconnected from the gas manifold.

Hydrothermal HDN reactions were carried out by placing the loaded and sealed reactors vertically in a preheated Techne Fluidized Sand Bath (model SBL-2). The reactor reached the sand bath set point temperature within 5 min. When the desired reaction duration had been reached, the reactors were removed from the sand bath and immersed in an ice water bath for about 5 min to stop the reaction. The reactors were further cooled in a refrigerator for 30 min. The reactors were then removed from the refrigerator and placed in ambient conditions for at least 15 h to allow the liquid–gas system to reach equilibrium prior to performing the gas-phase analysis. After analyzing the gas fraction, the reactors were cooled again and then the reactors were opened and tetrahydrofuran was added to recover the liquid fraction. The reactor contents were first transferred to a 10 ml volumetric flask. The reactor was then rinsed at least five times with tetrahydrofuran to ensure complete recovery of all material. Additional tetrahydrofuran was then added to the volumetric flask to bring the total volume to 10 ml.

2.3. Analytical chemistry

The reaction products were identified by an Agilent 5970 Mass Spectrometric (MS) detector and by matching gas chromatograph (GC) retention times with known standards. Routine quantification was done using a GC with flame ionization detector (FID). Separation of the liquid-phase products for both GC-MS and GC-FID analysis was achieved by using an Agilent 6890 GC equipped with a 30 m × 0.23 mm × 0.32 μm Alltech Heliflex®AT-CAM capillary column. The injection port temperature was 150 °C, and the oven temperature program consisted of a 4 min soak at 35 °C followed by an 8 °C min^{-1} ramp up to 150 °C, which was held for 22 min. Quantitative analysis was performed using experimentally determined calibration curves for each compound of interest. The FID response was linear for each component over the concentration ranges used.

The gas-phase products, except C_3–C_5 alkanes, were analyzed as previously described [7,8]. For the analysis of C_3–C_5 alkanes, an Agilent 6890N GC equipped with a thermal conductivity detector (TCD) was employed. We used a 6 ft × 2.1 mm I.D. × 1/8 in. O.D. stainless steel column, packed with 80/100 mesh Porapak Q (Supleco) to separate each component in the mixture. The temperature of the column was initially held at 35 °C for 5 min and then it increased to 225 °C at a rate of 20 °C min^{-1}. The final temperature was held for 15 min.

The concentration of ammonia in the aqueous samples was determined according to Standard Method 4500-NH_3 F [14]. Analysis of control samples with known concentrations of pyridine, piperidine, pentylamine, and 1-pentyl-piperidine indicated no interference of these pyridine HDN intermediate products with the ammonia analysis.

Table 1
Results from pyridine hydrothermal HDN (5.5 MPa H_2) with different catalysts under different conditions.

Run	Catalyst	Temperature (°C)	Time (h)	Catalyst loading (wt%)	Pyridine % conversion	C_{4+5} yield (%)
1	None	450	1	–	8 ± 2	0
2	Pt/C	250	4	50	99 ± 5	0.63 ± 0.06
3	Pd/C	250	4	50	100 ± 5	0.28 ± 0.03
4	Ru/C	250	4	50	100 ± 5	0.63 ± 0.05
5	Rh/C	250	4	50	100 ± 5	0.12 ± 0.01
6	Pt/C, sulfided	250	4	50	58 ± 3	0.20 ± 0.02
7	Pt/γ-Al_2O_3	250	4	50	69 ± 4	1.06 ± 0.11
8	CoMo/γ-Al_2O_3	250	4	50	16 ± 1	0.12 ± 0.01
9	Pt/C	350	4	100	99 ± 4	3.51 ± 0.32
10	Pd/C	350	4	100	100 ± 5	2.06 ± 0.21
11	Ru/C	350	4	100	100 ± 5	0.12 ± 0.01
12	Rh/C	350	4	100	100 ± 5	5.89 ± 0.48
13	Pt/C, sulfided	350	4	100	96 ± 5	7.09 ± 0.67
14	Pt/γ-Al_2O_3	350	4	100	95 ± 4	12.83 ± 1.18
15	Mo_2C	350	4	100	80 ± 4.	0.12 ± 0.01
16	MoS_2	350	4	100	33 ± 2	0.12 ± 0.01
17	Pt/C	400	1	100	100 ± 5	10.76 ± 0.54
18	Pd/C	400	1	100	98 ± 5	4.41 ± 0.23
19	Ru/C	400	1	100	100 ± 5	1.72 ± 0.08
20	Rh/C	400	1	100	100 ± 5	14.73 ± 0.74
21	Pt/C, sulfided	400	1	100	91 ± 4	21.75 ± 1.09
22	Pt/γ-Al_2O_3	400	1	100	100 ± 5	80.59 ± 3.89
23	CoMo/γ-Al_2O_3	400	1	100	53 ± 3	0.78 ± 0.04
24	PtO_2	400	1	100	94 ± 4	41.97 ± 2.14
25	Activated carbon	400	1	100	74 ± 4	2.35 ± 0.12
26	Al_2O_3	400	1	100	5.5 ± 0.3	0
27	Pt/γ-Al_2O_3	400	0.5	100	93 ± 5	60.53 ± 3.22
28	Pt/C, sulfided	400	0.5	100	84 ± 4	20.29 ± 1.01
29	PtO_2	400	0.5	100	82 ± 5	24.25 ± 1.22
30	Pt/γ-Al_2O_3	400	1.5	100	100 ± 5	73.42 ± 3.48
31	PtO_2	400	1.5	100	99 ± 5	55.07 ± 2.81
32	Pt/γ-Al_2O_3[a]	400	1.5	100	38 ± 2	0.20 ± 0.01

[a] 5.5 MPa N_2 was charged instead of H_2.

Pyridine conversion was evaluated as the number of moles of pyridine recovered divided by the initial number of moles of pyridine loaded into the reactor. Product molar yields were calculated as the number of moles of product recovered from the gas and liquid phases divided by the initial number of moles of pyridine loaded into the reactor. The uncertainty in the results was determined experimentally as the standard deviation from at least two independent experiments conducted under nominally identical conditions. Results reported herein represent the mean values for the independent trials.

3. Results and discussion

This section presents and interprets the experimental results from pyridine HDN in supercritical water. We first screened different catalysts with the intent of selecting the most active for more detailed studies. This catalyst, Pt/γ-Al_2O_3, was then used in experiments to elucidate the influence of process variables (e.g., temperature, time, catalyst loading, initial hydrogen pressure, and water density) on hydrothermal catalytic HDN. A reaction scheme for the HDN of pyridine under hydrothermal conditions is also proposed.

3.1. Background experiments

To determine whether the thermal decomposition of pyridine was significant at the selected reaction conditions, we conducted a neat pyrolysis experiment in a helium atmosphere at 420 °C, the highest temperature used in the present HDN experiments. No hydrogen, water, or catalyst was added to the reactor. After 90 min at 420 °C, 90 ± 5% of pyridine remained unreacted. A second control experiment was done to determine the extent of pyridine hydrolysis in SCW. After 60 min at 450 °C (w/ρ_w = 0.10 g/cm^3), 92 ± 2% of the pyridine remained unreacted. These results indicate that the thermal and or hydrolytic decomposition of pyridine would be expected to contribute conversions of a few percent, at most, under the conditions we investigated. This outcome is in agreement with an earlier report on the stability of pyridine in SCW [15]. Finally, we subjected pyridine to SCW at 450 °C for 1 h under high-pressure H_2 (in the absence of any catalysts) and observed no C_4 or C_5 compounds, which are the main HDN products. This experiment indicates that the C_4 and C_5 detected in the HDN experiments arose exclusively from catalytic reactions. These background experiments demonstrate that the results obtained in the catalytic experiments are due to catalytic HDN and not to some competing thermal or hydrothermal reaction path.

3.2. Catalyst screening for hydrothermal HDN of pyridine

Initial work focused on testing the influence of different materials on the hydrothermal HDN of pyridine under different reaction conditions. Table 1 displays the catalysts and conditions used in this initial catalyst screening work. The pyridine loading was 0.1 ml in each experiment.

On the basis of being the major HDN products, the n-butane (C_4) and n-pentane (C_5) yields provide a good indicator of overall HDN catalytic activity. Therefore, we used the sum of these molar yields (denoted by C_{4+5}) to evaluate the activities of several different materials toward the hydrothermal HDN of pyridine. Table 1 shows the C_{4+5} yields from experiments with different catalysts at different temperatures and reaction times. All of the materials tested showed some activity for HDN. Pt/C showed only modest activity toward C_{4+5} production (Runs 2, 9, 17), and the HDN activity was usually higher when using the sulfided form of this catalyst (Runs 13, 21, 28). Activated carbon itself also has some catalytic activity for HDN (Run 25), but it is much less than that of the noble metals it supports in the other catalysts. Among the carbon-supported

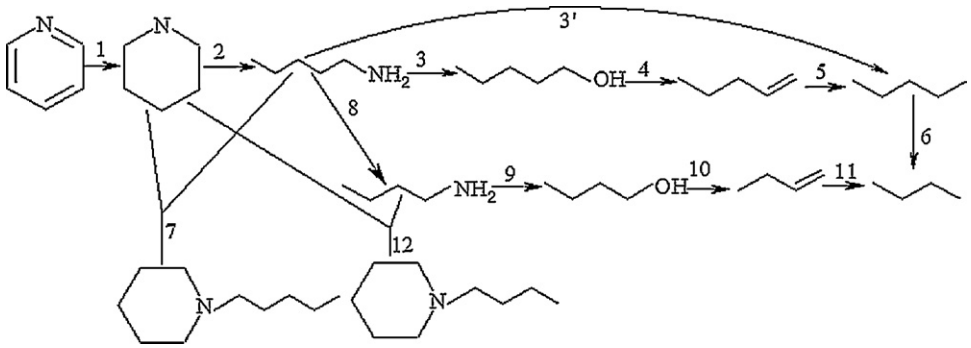

Fig. 1. Reaction network for pyridine HDN under hydrothermal conditions.

metal catalysts, at 350 and 400 °C, Ru/C shows the lowest yields of C_{4+5} (Runs 11,19). This result is consistent with literature showing that Ru is a very effective catalyst for hydrothermal gasification [16] under these conditions. Gasification of pyridine and its HDN products would compete favorably with HDN and thereby reduce the yields of the HDN products. CoMo/γ-Al_2O_3, an effective HDN catalyst in organic solvents, performed poorly for pyridine HDN under hydrothermal conditions (Run 8, 23). We note, however, that the catalyst is maintained in its reduced sulfide form when used in organic media whereas we made no attempt to do so in this work because of the desire to identify catalysts that would be active even in an oxidizing hydrothermal environment. Bulk PtO_2 showed appreciable activity for HDN (Runs 24, 29, 31) in supercritical water. It is possible that the oxide was converted to Pt(0) under the reducing reaction conditions, in which case metallic Pt would be the catalytic species. This behavior has been reported in previous studies with PtO_2 in SCW [17]. Of all the catalysts tested, however, 5% Pt/γ-Al_2O_3 consistently gave the best overall performance for the HDN of pyridine under various sets of hydrothermal reaction conditions (Runs 7, 14, 22, 27, 30). C_{4+5} yields of 70–80% were obtained, whereas no other catalyst produced yields exceeding 55%. The alumina support itself was inactive for HDN (Run 26). Without high-pressure H_2 in the reactor, almost no C_4 and C_5 were detected even in the presence of Pt/γ-Al_2O_3 (Run 32). Given the activity of PtO_2 in these experiments, it seems that a catalyst support is not required for HDN activity. The literature [22] suggests, however, that the Al_2O_3 support might be involved in breaking the C–N bond, which could explain why the Pt/γ-Al_2O_3 catalyst was more active than Pt/C.

3.3. Hydrothermal HDN products and pathways over Pt/γ-Al_2O_3

Having identified Pt/γ-Al_2O_3 as the most active catalyst (among those tested) for hydrothermal HDN of pyridine, we next discuss the numerous reaction products that formed under the wide variety of reaction conditions examined. The product spectrum from hydrothermal HDN of pyridine was both complex and condition dependent. At the mildest conditions investigated (250 °C or short reaction times), the most abundant products were piperidine and its alkyl substituted derivatives (e.g., 1-pentyl-piperidine and 1-butyl-piperidine). This result indicates that hydrogenation of pyridine is the dominant primary reaction path, and that little N removal occurs initially. Indeed, Table 1 shows that pyridine conversions of essentially 100% were achieved at 250 °C, but that the yield of HDN products was less than 1%. At higher temperatures or longer reaction times, the most abundant products are n-butane and n-pentane, suggesting that hydrogenolysis of the initial hydrogenation products is the predominant reaction. Increasing the temperature increases the overall C_{4+5} yields. These observations are consistent with the behavior of this reaction in organic media over conventional hydrotreating catalysts, where the HDN of pyridine occurs through sequential hydrogenation and hydrogenolysis steps [18]. In addition to these products, a large number of other products were also identified from the hydrothermal HDN of pyridine. These other products included n-pentylamine, n-pentanol, and 1-pentene. Fig. 1 shows that these products can be expected as intermediates along the main reaction path for hydrothermal HDN of pyridine over Pt/γ-Al_2O_3. We constructed Fig. 1 on the basis of our results and previous studies on pyridine HDN.

Steps 1–5 are the main reaction paths in the HDN network. The first reaction path involves hydrogenation of the heterocyclic ring to form piperidine, which then undergoes C–N bond hydrogenolysis to form n-pentylamine in step 2. Two parallel reaction pathways are available for pentylamine in this hydrothermal environment: hydrolysis to form n-pentanol and ammonia (step 3) or hydrogenolysis to form pentane and ammonia (step 3′). The n-pentanol formed in step 3 can then undergo dehydration to form n-pentene and subsequent hydrogenation to give n-pentane. The reactivity of n-pentylamine is high relative to that of pyridine and piperidine, especially at low temperatures [19].

Apart from the main reactions, there exist some side reactions. Piperidine can react with pentylamine to form 1-pentyl-piperidine (step 7) at lower temperatures [20] via the amine disproportionation reaction [21,22]. The structural similarity between 1-pentyl-piperidine and 1-butyl-piperidine suggests that their formation mechanisms are also similar. That is, 1-butyl-piperidine can be produced through piperidine reacting with butylamine. Step 12 shows this reaction. Butylamine is probably formed by cracking a

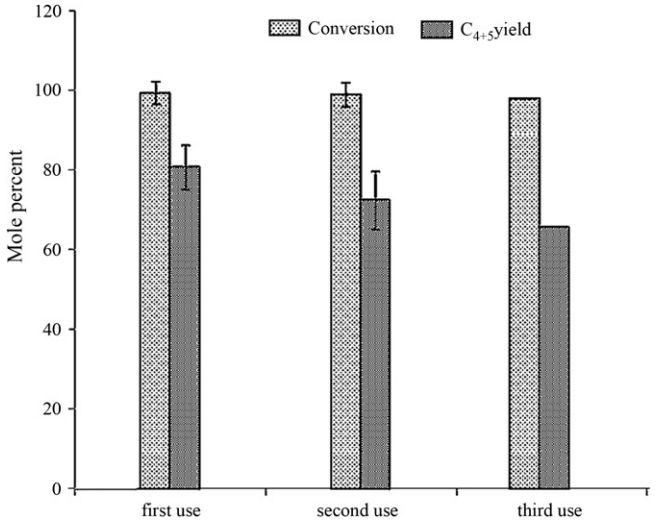

Fig. 2. Pyridine conversion and C_{4+5} yield from pyridine denitrogenation with catalyst after first, second, and third use.

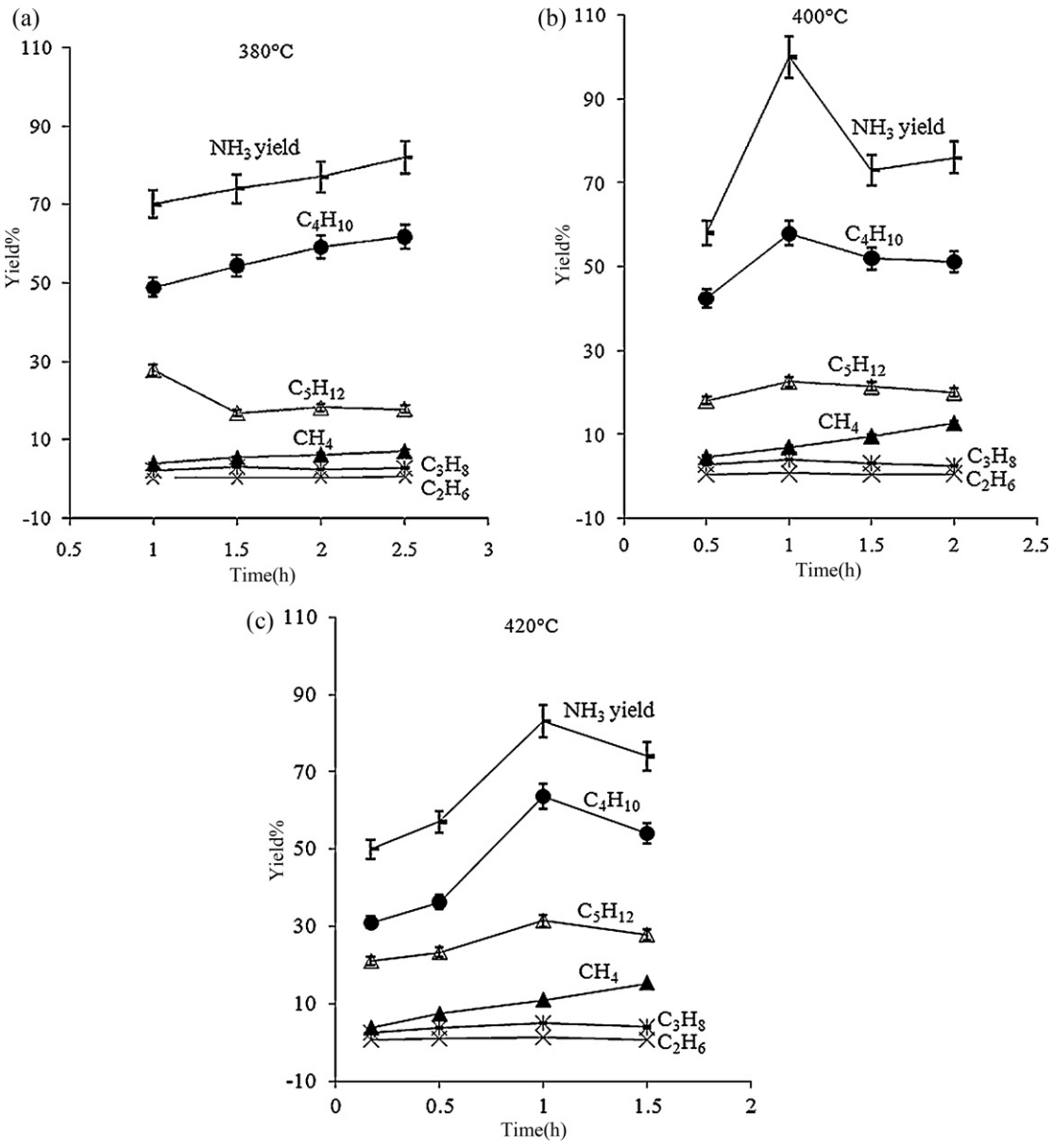

Fig. 3. (a) Temporal variation of product yields from pyridine HDN over Pt/γ-Al_2O_3 at 380 °C. (b) Temporal variation of product yields from pyridine HDN over Pt/γ-Al_2O_3 at 400 °C. (c) Temporal variation of product yields from pyridine HDN over Pt/γ-Al_2O_3 at 420 °C.

carbon atom from n-pentylamine (step 8) [23]. Butane, one of the main hydrocarbon products, could be produced through rupture of the C–N bond in butylamine as shown in steps 9, 10 and 11. Another possible pathway for the formation of butane is the cracking of n-pentane (step 6). The presence of a significant amount of C_1–C_3 alkanes in the gaseous products is consistent with the occurrence of cracking reactions.

3.4. Catalyst activity maintenance

Pt supported on γ-alumina was the most active catalyst for hydrothermal HDN of pyridine, but the support is known to undergo a phase transition to α-alumina in SCW, which leads to a reduction in surface area [24]. To learn the extent to which this phase transition would affect the activity of Pt/γ-Al_2O_3 as an HDN catalyst in a hydrothermal environment, we conducted experiments probing the activity of this catalyst when re-used. Activity maintenance was determined by employing again in a new HDN experiment the catalyst recovered from a reactor at the end of a previous run. Each hydrothermal HDN run was done at 400 °C for 1 h with 0.1 g of catalyst and 0.1 g of pyridine. The new run was in a different batch reactor with a fresh loading of pyridine and water, but with a previously used catalyst. The activity was assessed by measuring both the pyridine conversion and the yield of C_{4+5}.

Fig. 2 shows the pyridine conversion and C_{4+5} yield from HDN of pyridine with fresh Pt/γ-Al_2O_3 (1st use), with catalyst used once previously (2nd use), and with catalyst used twice previously (3rd use). There are no error bars on the data for the third use of the catalyst because we recovered an insufficient amount of catalyst from the second use to do replicates for this final condition. The conversion of pyridine was essentially complete in all runs, but the yield of C_{4+5} products showed a modest decrease from 81% with fresh catalyst to 65% with the twice-used catalyst. Previous work on oxidation reactions in SCW with Al_2O_3 supported catalysts also showed that activity was largely maintained even though the catalyst support underwent morphological changes [24]. Aki and Abraham speculated that the redispersion of Pt metal on the support in SCW may have helped to maintain the catalyst activity,

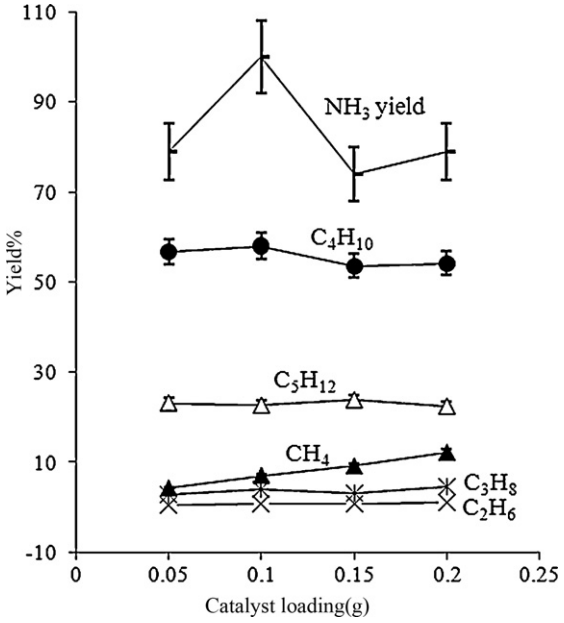

Fig. 4. Effect of Pt/γ-Al_2O_3 loading on pyridine hydrodenitrogenation in SCW (400 °C, 1 h).

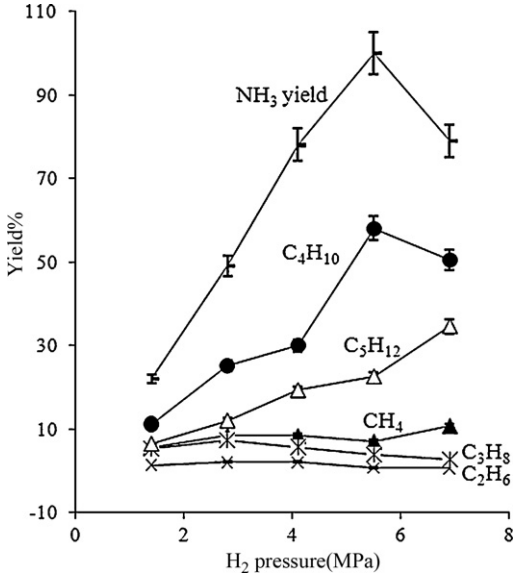

Fig. 5. Effect of hydrogen loading (P at room temp) on HDN of pyridine in SCW (400 °C, 1 h).

even while the catalyst support underwent a phase transition [25]. Additional work is required to understand more fully catalyst deactivation in this system.

3.5. Effect of temperature and reaction time

Fig. 3 shows the temporal variation of the yields of HDN products from hydrothermal treatment of pyridine over Pt/γ-Al_2O_3 at 380, 400, and 420 °C. The most abundant products of pyridine HDN at these conditions are butane, pentane, methane, propane, and ethane. The nitrogen was removed in the form of ammonia. Carbon oxides were present at low levels even though the residual air was removed from the reactor prior to the reaction. CO and CO_2 can be formed from reactions such as steam reforming and water-gas shift. The highest yields of butane (64%) and methane (15%) were realized at reaction times of 1 h and 1.5 h at 420 °C, respectively. Methane could be formed via the methanation reaction, but it can also arise from cracking of higher hydrocarbons. C_2, C_3, C_4 might also come from the cracking of C_5 at higher temperatures. The highest yield of pentane (32%) was obtained at a reaction time of 1 h at 420 °C.

Fig. 3 shows that the yields of light gases (C_1–C_3) generally increase with time and with temperature. This result is consistent with these products arising from cracking of the main C_4 or C_5 HDN product. These reactions would be undesirable as they increase the gas make at the expense of larger molecules.

Fig. 3 also shows the NH_3 yields measured in these experiments. Since NH_3 is the ultimate product from pyridine HDN, the yield of NH_3 is a direct measure of the extent of N removal from pyridine. The calculation of the ammonia yield includes NH_3 quantified in both the aqueous and gas phases. Increasing the reaction time generally leads to higher NH_3 yields, and hence increased HDN. N removal routinely exceeded 70% under the experimental conditions of Fig. 3.

3.6. Effect of catalyst loading

Fig. 4 shows the effect of catalyst loading on the HDN product distribution at 400 °C for 1 h with 0.1 ml pyridine loading. It is clear that the butane and pentane yields are essentially independent of the catalyst loading over the range investigated. It seems that maximal yields of HDN products could have been obtained with even lower catalyst loadings, which is a desirable feature for an HDN catalyst. A modestly higher yield of NH_3 was obtained at a catalyst loading of 0.1 g, but it is not clear that the high yield is statistically significant given the experimental uncertainties shown.

3.7. Effect of initial hydrogen pressure

Hydrogen plays two major roles in HDN. The first is to hydrogenate the unsaturated heterocyclic ring and the second is to hydrocrack the subsequent products. An increase in hydrogen pressure favors both of these steps. We investigated the effect of initial hydrogen pressure on the product yields from pyridine HDN in SCW (400 °C for 1 h with 0.1 ml pyridine). Fig. 5 shows that the hydrogen pressure strongly affects the NH_3 yield and product distribution. The yield of NH_3 increased with an increase of the initial hydrogen pressure from 1.4 MPa to 5.5 MPa. A further increase in the initial hydrogen pressure led to a modest decline in the NH_3 yield. At lower initial hydrogen pressure, where less HDN had occurred, the reaction products are largely alkyl substituted pyridines such as 2-methyl-pyridine, 2-propyl-pyridine and 2-pentyl-pyridine and dehydration products such as 2,2′-bipyridine and 2,3-bipyridine.

Fig. 5 shows that the yield of pentane increases with increasing hydrogen pressure. The highest yield (35%) was obtained at an initial hydrogen pressure of 6.9 MPa. Increasing initial hydrogen pressure also increases the butane yield when going from 1.4 to 5.5 MPa. The highest yield (58%) was obtained at an initial hydrogen pressure of 5.5 MPa. It is not clear that the difference between the two yields at the two highest pressures are statistically significant. The yields of C_2 and C_3 decrease with increasing H_2 pressure, suggesting that pressure inhibits the cracking reactions.

The results in Fig. 5 can be understood on the basis of the reaction stoichiometry, kinetics, and thermodynamics. The experiments at $P_{H_2} < 4.3$ MPa were substoichiometric in H_2. The amount of H_2 in the reactor corresponded to 0.33, 0.65, 0.95, 1.28 and 1.60 of the stoichiometric requirement for HDN at 1.4, 2.8, 4.1, 5.5 and 6.9 MPa, respectively. Stoichiometry alone did not limit the NH_3 and C_4 and C_5 yields, however, as the yields were always below these stoichiometric limits. Thus, it appears that kinetics also plays a role. The hydrogenation step likely becomes faster as more H_2 is present

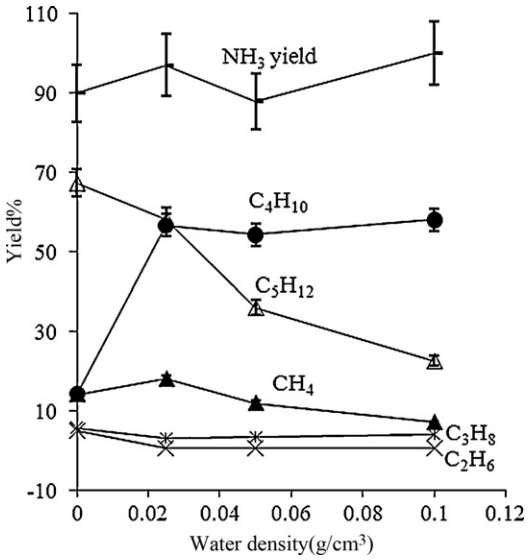

Fig. 6. Effect of water density on HDN of pyridine (400 °C, 1 h).

in the reactor. Higher H_2 pressure also favors HDN by shifting the equilibrium for the initial piperidine formation step to the right.

3.8. Effect of water density

The water density was varied while keeping other process variables fixed to probe its effect on pyridine HDN. Fig. 6 shows the experimental results (400 °C, 60 min), which indicate very little effect of density on the NH_3 yield. This yield exceeded 90% at all densities investigated. Unlike the absence of any marked effect on NH_3 yield, Fig. 6 shows that the presence of water significantly affects the HDN product yields. In the absence of water, the major product is pentane and its yield here (67%) is the highest observed in any of our experiments. The pentane yield decreases steadily as the water density increases from 0 to 0.1 g/cm^3. The butane yield increases to 57% with an increase in water density from 0 to 0.025 g/cm^3. Further increases in water density have little effect on the butane yield. The highest total C_{4+5} yield was obtained at a water density of 0.025 g/cm^3. This yield was almost 100%, the NH_3 yield was almost 100%, and the pyridine conversion was also almost 100%. Thus, at this water density we achieved essentially 100% yields of and selectivity to the HDN products. Therefore, from a yield and selectivity perspective, a 0.025 g/cm^3 water density seems to be preferred to both higher water densities and to the absence of water. The yields of C_1, C_2 and C_3 decrease with increasing water density.

The results in Fig. 6 show clearly that performing HDN of pyridine in SCW leads to a very different product distribution than does HDN in the absence of water. The reason for this marked difference is not clear, but we suspect it is related to the presence of water providing a new reaction path (e.g., hydrolysis of pentylamine) that is unavailable in its absence. Thus, the major catalytic reaction paths in SCW appear to differ from those in organic media. This finding reinforces the need for investigations into hydrothermal HDN, such as the present study.

4. Conclusions

5% Pt/γ-Al_2O_3 catalyzes the hydrothermal HDN of pyridine to produce hydrocarbons. The catalyst can be reused up to at least three times with only modest loss in HDN activity. The main products of pyridine HDN in SCW are n-butane and n-pentane. The proportion of n-pentane among the HDN products decreased as the water density increased. In the absence of water, n-pentane was the major HDN product, whereas in the presence of SCW, n-butane was more abundant. Thus it seems clear that the presence of water influences the HDN pathways. Hydrogen plays an important role in pyridine HDN in SCW, but only a modestly superstoichiometric H_2/pyridine ratio (6.5:1) is required for essentially complete nitrogen removal from pyridine. Performing the HDN reaction at 400 °C, 1.0 h, 0.025 g/cm^3 water density, 5.5 MPa H_2 and 100% catalyst loading led to complete conversion of pyridine to hydrocarbon products. Thus, this work shows that nitrogen in pyridine can be effectively removed in SCW in the presence of a Pt/γ-Al_2O_3 catalyst and high-pressure H_2.

Acknowledgements

We gratefully acknowledge financial support from the University of Michigan College of Engineering and from the U.S. National Science Foundation (EFRI-0937992). P. Duan acknowledges the financial support from Henan Polytechnic University (B2011-008).

References

[1] T. Brown, P. Duan, P.E. Savage, Energy Fuel 24 (2010) 3639–3646.
[2] P. Duan, P.E. Savage, Ind. Eng. Chem. Res. 50 (2011) 52–61.
[3] A.B. Ross, P. Biller, M.L. Kubacki, H. Li, A. Lea-Langton, J.M. Jones, Fuel 89 (2010) 2234–2243.
[4] D. Zhou, L. Zhang, S. Zhang, H. Fu, J. Chen, Energy Fuel 24 (2010) 4054–4061.
[5] P.E. Savage, Chem. Rev. 99 (1999) 603–622.
[6] M.C. Clark, B. Subramaniam, AIChE J. 45 (1999) 1559–1565.
[7] P. Duan, P.E. Savage, Bioresour. Technol. 102 (2011) 1899–1906.
[8] P. Duan, P.E. Savage, Energy Environ. Sci. 4 (2011) 1447–1456.
[9] P.E. Savage, J. Supercrit. Fluids 47 (2009) 407–414.
[10] P.-Q. Yuan, Z.-Mi. Cheng, X.-Y. Zhang, W.-K. Yuan, Fuel 85 (2006) 367– 373.
[11] P.-Q. Yuan, Z.-M. Cheng, W.-L. Jiang, R. Zhang, W.-K. Yuan, J. Supercrit. Fluids 35 (2005) 70–75.
[12] T. Adschiri, R. Shibata, T. Sato, M. Watanabe, K. Arai, Ind. Eng. Chem. Res. 37 (1998) 2634–2638.
[13] B.M. Vogelaar, M. Makkee, J.A. Moulijn, Fuel Process. Technol. 61 (1999) 265–277.
[14] L.S. Clesceri, A.E. Greenberg, A.D. Eaton, Standard methods for the examination of water and wastewater, 20th ed., Am. PublicHealth Assoc., Washington, DC, 1998.
[15] A.R. Katritzky, R.A. Barcock, Energy Fuel 8 (1994) 990–1001.
[16] D.C. Elliott, Biofuel, Bioprod. Biorefin. 2 (2008) 254–265.
[17] R.C. Crittendon, E.J. Parsons, Organometallics 13 (1994) 2587–2591.
[18] H.G. Mcllvries, Ind. Eng. Chem. Process Des. Dev. 10 (1971) 125–130.
[19] V. Schwartz, S.T. Oyama, J. Mol. Catal. A: Chem. 163 (2000) 269–282.
[20] J. Sonnemans, G.H. Van der Berg, P. Mars, J. Catal. 31 (1973) 220–230.
[21] J. Sonnemans, F. Goudriaan, P. Mars, The hydrogenolysis of pyridine on molybdenum oxide containing catalysts, in: Paper 76, Fifth Intl. Cong. on Catal., Palm Beach, FL, 1972.
[22] F. Goudriaan, Hydrodenitrogenation of Pyridine, doctoral thesis, Twente Technical Institute, The Netherlands, 1974.
[23] Y. Chu, Z. Wei, S. Yang, C. Li, Q. Xin, E. Min, Appl. Catal. A: Gen. 176 (1999) 17–26.
[24] J. Yu, P.E. Savage, Appl. Catal. B: Environ. 28 (2000) 275–288.
[25] S. Aki, M.A. Abraham, Ind. Eng. Chem. Res. 38 (1999) 358–367.